Catal Lett (2009) 129:422–427
DOI 10.1007/s10562-008-9814-9

Relationship Between the Structure of Manganese Oxides on Alumina and Catalytic Activities for Benzene Oxidation with Ozone

Hisahiro Einaga · Masafumi Harada · Atsushi Ogata

Received: 17 October 2008 / Accepted: 2 December 2008 / Published online: 9 January 2009

Abstract Catalytic oxidation of benzene with ozone was carried out over alumina-supported manganese oxides. Manganese oxides was highly dispersed on alumina at low loading levels (Mn <2.5 wt%) and aggregated Mn_3O_4 crystallites were formed at the high loading levels (>7.5 wt%). Both the Mn oxide species were active for benzene oxidation with ozone, and the former showed slightly higher activities. TPO studies of used catalysts revealed that the oxidation behavior of benzene was not so much influenced by the Mn loadings.

Keywords Manganese oxides · Alumina support · Catalytic oxidation · Ozone · Benzene

1 Introduction

Control of VOCs has been one of the important topics in the research area of environmental catalysis. Catalytic oxidation by using ozone (catalytic ozonation) is one of the useful methods for the treatment of flue gases polluted with volatile organic compounds (VOCs), especially at their low concentration levels [1]. So far, catalytic ozonation has been studied for the oxidation of various types of VOCs including benzene [2–7], ethanol [8], acetone [9], and cyclohexane [10]. As for the catalysts, supported manganese oxide catalysts have been frequently studied for catalytic ozonation of VOCs [6–13] and they showed the highest activities for benzene oxidation among the oxides of metal in the first transition series [6]. We have reported the oxidation behavior of benzene and cyclohexane with ozone on alumina-supported manganese oxide ($MnOx/\gamma$-Al_2O_3) catalysts [7, 10]. These organic compounds were decomposed to CO_2 and CO and partially oxidized byproducts such as weakly bound compounds and strongly bound surface species were formed on the catalysts [7]. Although the build-up of these byproducts on catalyst surface causes the catalyst deactivation, subsequent heat treatment can regenerate the deactivated catalyst.

Our previous studies have shown that manganese is crucial to obtaining the catalytic activity and support materials without Mn species exhibit almost no activities for catalytic ozonation of benzene and cyclohexane [7]. Oyama and his coworkers have revealed that the role of Mn species is to decompose ozone to form the active oxygen species that are active for VOC oxidation [11–13]. Despite of the significance of Mn, little information has been known on the active sites for catalytic ozonation of benzene. In this study, the $MnOx/\gamma$-Al_2O_3 catalysts with varying Mn dispersions were prepared and used for benzene oxidation with ozone. Numerous papers have been published on $MnOx/\gamma$-Al_2O_3, reporting that their structures strongly depend on the preparation method [14]. The impregnation method with acetate precursor enabled us to prepare the catalysts having different Mn structures. The

H. Einaga (✉)
Department of Energy and Material Sciences,
Faculty of Engineering Sciences, Kyushu University,
Kasuga, Fukuoka 816-8580, Japan
e-mail: einaga@mm.kyushu-u.ac.jp

M. Harada
Department of Health Science and Clothing Environment,
Faculty of Human Life and Environment, Nara Women's
University, Nara 630-8506, Japan

A. Ogata (✉)
Institute for Environmental Management Technology,
National Institute of Advanced Industrial Science
and Technology (AIST), AIST Tsukuba West, 16-1,
Onogawa, Tsukuba, Ibaraki 305-8569, Japan
e-mail: atsushi-ogata@aist.go.jp

structures of Mn oxides were investigated by using XRD, Raman, and EXAFS. The relationship between the Mn oxide structures and the catalytic activities gave us important information on the active sites on MnOx/γ-Al_2O_3 catalysts for benzene oxidation with ozone.

2 Experimental

2.1 Catalyst Preparation

Alumina-supported manganese oxides were prepared by impregnation of γ-Al_2O_3 (Catalysis Society of Japan JRC ALO-8, $S_{BET} = 168\ m^2\ g^{-1}$) with aqueous solutions of $Mn(CH_3COO)_2{\cdot}4H_2O$ (Wako Pure Chemical, >99.9%). The catalyst samples were then dried at 383 K for 24 h and calcined at 773 K for 3 h in air. The impregnation was performed in several steps according to the reported procedures [14]. MnO, Mn_2O_3, Mn_3O_4, and MnO_2 were purchased from Aldrich and used as reference samples without further purification.

2.2 Catalyst Characterization

XRD patterns were measured by using a Rigaku XRD diffractometer RU-200 using Co-Kα radiation. The X-ray tube was operated at 30 kV and 100 mA. Raman spectra were taken in the spectral range of 200–800 cm^{-1} by using a Jasco NRS-1000 spectrometer equipped with a CCD detector. The 532 nm line from Yttrium–aluminum–gallium (YAG) laser (green laser) was used as the excitation source. Catalyst samples were pressed into pellets with 20 mmϕ in diameter. Prior to these measurements, the catalyst samples were heated at 723 K in O_2 flow for 3 h.

2.3 EXAFS Studies

EXAFS measurements were carried out at the Photon Factory beam line BL-7C in high energy accelerator research organization (KEK-PF) with the storage ring operating at an energy of 2.5 GeV. The double crystal monochromator Si(111) was used. Catalyst samples were pressed into thin self-supporting wafers with 20 mmϕ in diameter. These samples were heated at 723 K in O_2 flow for 2 h, and then sealed in Ar with polyethylene film without contact with air. The incident and transmitted X-rays were detected by N_2-filled ionization chambers. XAFS spectra were recorded at a temperature of 296 K. Data reduction of experimental absorption spectra was carried out according to the method recommended by the standards and criteria committee of the international XAFS society [15] using WinXAS v.3.1 [16, 17].

2.4 Catalytic Reactions

Catalytic reactions were carried out with a fixed bed flow reactor. Details of the reaction systems are described elsewhere [7]. Ozone was synthesized from O_2 by a silent discharge ozone generator. Prior to the catalytic reaction, the sample in a Pyrex glass reactor was heated at 723 K in O_2 flow. Then, the catalyst was cooled and thermostated at 295 K with a water bath. After the adsorption–desorption equilibriun was achieved for benzene between the catalyst surface and gas phase, ozone was continuously fed to the reactor. Analysis of gas sample was performed with a Fourier-transform infrared spectrophotometer (Perkin-Elmer Spectrum One) equipped with a 2.4 m optical length gas cell (volume 100 mL). In this system, homogeneous gaseous reaction of benzene with ozone can be neglected [7]. Reaction rates were evaluated under the conditions where the conversions were linear to W/F.

3 Results and Discussion

3.1 Structure of Alumina-Supported Manganese Oxides

Figure 1 shows the XRD patterns of MnOx/γ-Al_2O_3 catalysts with various Mn loadings. For the catalyst samples with Mn loadings below 5%, only the diffraction patterns due to γ-alumina were observed, implying that manganese oxides were highly dispersed on the support material. As

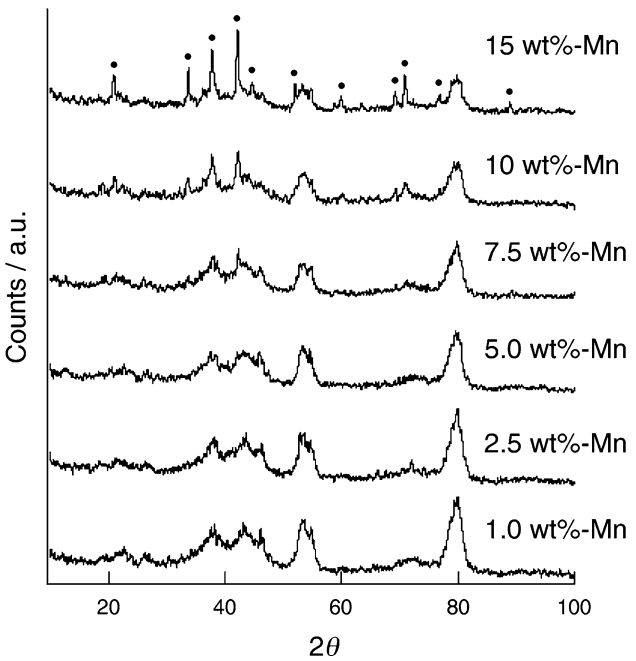

Fig. 1 XRD patterns of the MnOx/γ-Al_2O_3 catalysts. The dots (•) refer the Mn_3O_4 phase

Table 1 BET surface area of MnOx/γ-Al_2O_3 catalysts

Mn loading (wt%)	Surface area[a] (m^2 g^{-1})
–	168
1.0	163
2.5	162
5.0	156
7.5	151
10.0	147
15.0	136

[a] Catalyst samples were evacuated at 573 K for 3 h prior to the BET measurements

the Mn loadings increased to higher loading level (10–15%), the diffraction patterns of crystalline Mn_3O_4 appeared and their intensities increased. The other crystal phases such as MnO, MnO_2, and Mn_2O_3 were not observed. BET surface area of alumina-supported manganese oxides decreased with increasing Mn loading, as shown in Table 1, coincident with the formation of Mn_3O_4 crystalline.

Figure 2 shows the Raman spectra of MnOx/γ-Al_2O_3 catalysts. The catalyst samples with low Mn loadings (1–5 wt%) gave only a broad peak at around 654 cm^{-1}, assignable to the highly dispersed manganese oxides on the support. As the Mn loading increased (10–15 wt%), the peaks at 318 and 370 cm^{-1} newly appeared and the intensities of the peaks around 654 cm^{-1} increased, indicating the formation and growth of Mn_3O_4 phase. It has been pointed out that Raman spectra may overemphasize

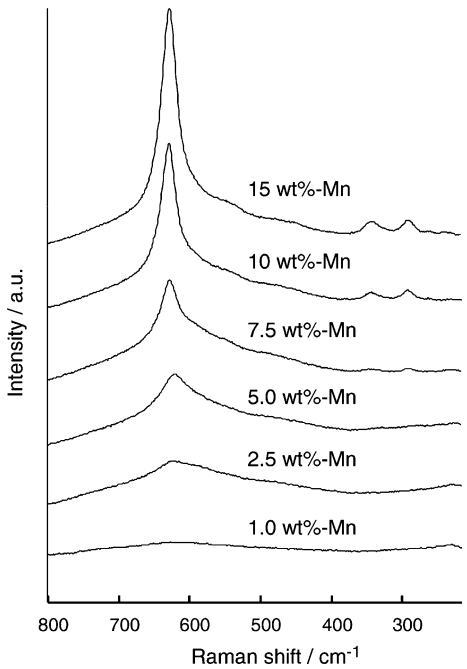

Fig. 2 Raman spectra of the MnOx/γ-Al_2O_3 catalysts

Mn_3O_4 phase because it is strongly Raman active compared with other manganese oxide phases. However, our spectra are consistent with the observations from XRD studies described above. No changes were observed for all the samples after the repetition of the measurements several times, excluding the possibility that manganese oxide phases were transformed by local heating with laser irradiation [18].

EXAFS spectra give us detailed information on the local structure of manganese oxides on alumina. Figure 3 shows the Mn–K edge Fourier transformed EXAFS spectra of MnOx/γ-Al_2O_3 catalysts with various loading level, along with four reference samples (phase uncorrected). At the Mn loading of 1 and 2.5 wt%, only a peak due to the bond of Mn–O was observed around 1.5 Å. On the other hand, the peaks in the range 2.5–3.5 Å appeared at high loading levels (5–15 wt%), which were mainly due to the contribution of Mn–Mn bond. Their intensities increased with increasing the Mn loading, while the peak for Mn–O was almost unchanged in their intensities. Thus, Mn species was highly dispersed at the loading levels (1.0 and 2.5 wt%), and the amount of Mn–O–Mn linkages increased with increasing the Mn loading level, leading to the formation of aggregated manganese oxides. The position and shape of the peaks for Mn–Mn contribution of MnOx/γ-Al_2O_3 (2.5 and 3.5 Å) was the same as that of Mn_3O_4 reference sample, supporting the results of XRD and Raman studies that Mn_3O_4 phase was formed at high Mn loading levels.

Kapteijin et al. [14] have reported that the structure of manganese oxide phase strongly depends on the precursors used in impregnation process: the acetate precursor resulted mainly in a highly dispersed surface manganese oxide phase, homogeneously distributed throughout the alumina particles. The local structures of MnOx/γ-Al_2O_3 catalysts prepared from acetate precursor have been also studied. EXAFS and Raman spectroscopy coupled with complementary ab initio calculations suggested that the structure of the manganese in MnOx/γ-Al_2O_3 was likely a four coordinate mononuclear species [19]. ESR studies revealed that all the manganese is present as isolated species at low loading levels, while the fraction of the isolated Mn species decreased with increasing the Mn loadings [20]. These results are in good agreement with our finding obtained from XRD, Raman, and EXAFS studies and clarified the structures of manganese oxides on alumina support. Manganese is present at isolated Mn species at low Mn loading (1.0–2.5 wt%). At higher loading level, the fraction of aggregated Mn oxides (5.0–7.5 wt%) increases. Further loading of Mn gives rise to the formation of Mn_3O_4 crystallite (10–15 wt%). Thus, the dispersion of Mn oxides can be easily controlled by changing the Mn loadings on alumina support by conventional impregnation method using manganese acetate as the catalyst precursor.

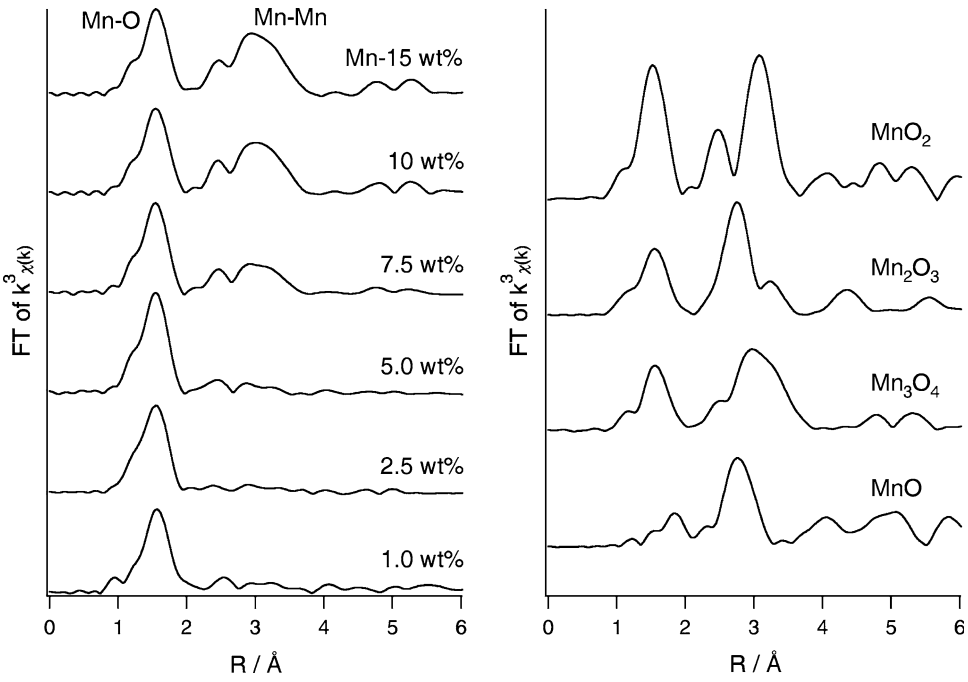

Fig. 3 Mn–K edge Fourier transformed EXAFS spectra of MnOx/γ-Al_2O_3 catalysts and manganese oxides as references

3.2 Catalytic Ozonation of Benzene Over MnOx/γ-Al_2O_3 Catalysts

Figure 4 shows the effect of Mn loading on the rate for benzene oxidation at 295 K. The rates were evaluated after 2 h and normalize by specific surface area. The alumina support without Mn showed almost no activities for benzene oxidation, as reported earlier [7]. The rate for benzene oxidation was slightly high at low loading levels (1–2.5 wt%) compared with the catalyst with high loading levels (5–15 wt%). However, no strong dependence was observed for the reaction rate and there was a plateau at high loading level where the fraction of aggregated Mn oxides increased with Mn loadings. These dependencies revealed that not only the highly dispersed Mn oxides but also the aggregated Mn oxides were the active sites for benzene oxidation with ozone. In a separate experiment, we confirmed that unsupported Mn_3O_4 also showed the catalytic activities for the benzene oxidation (data are not shown).

It has been reported that ozone decomposed to O_2 on supported manganese oxide catalysts as expressed by Eqs. (1–3), where * denotes active sites on the catalyst [11, 21, 22].

$$O_3 + * \rightarrow O_2 + O^* \quad (1)$$

$$O^* + O_3 \rightarrow O_2 + O_2^* \quad (2)$$

$$O_2^* \rightarrow O_2 + * \quad (3)$$

Kinetic studies and in situ Raman studies have revealed that the oxygen species O_2^* formed in this process are the active species for oxidation of organic compounds. Our previous study suggested that molecular oxygen was involved in the autoxidation reaction in which radical intermediates ($R^\bullet$) were oxidized by O_2 form final products, CO_2 and CO (autoxidation process) [7].

$$R^\bullet + O_2 \rightarrow RO_2^\bullet \rightarrow\rightarrow\rightarrow CO_2, CO \quad (4)$$

Here, $R^\bullet$ denotes radical intermediates formed in benzene oxidation. When the amount of O_2 involved in autoxidation processes increased, the ratio of ozone decomposition to benzene oxidation increased. In this

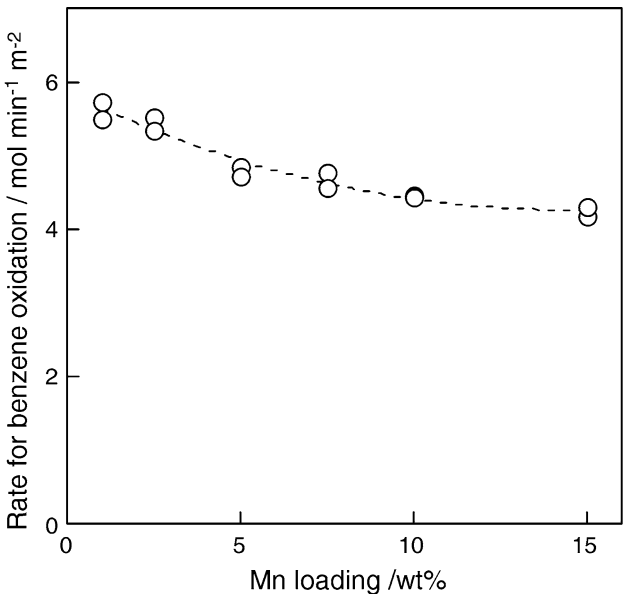

Fig. 4 Effect of Mn loading on the rate for catalytic ozonation of benzene over MnOx/γ-Al_2O_3 catalysts. Benzene 100 ppm, ozone 1,000 ppm, O_2 10%

study, the ratio of the rate for ozone decomposition to benzene oxidation was approximately 6 for all the MnOx/Al_2O_3 catalysts, implying that the oxidation process in catalytic ozonation of benzene was not so much affected by the Mn loadings.

Temperature programmed oxidation (TPO) of the used catalysts gave us the information on the byproduct compounds formed on the MnOx/Al_2O_3 catalysts in benzene oxidation. Heating the catalyst in O_2 flow resulted in the formation of CO_2 and CO due to the oxidation of byproduct compounds and desorption of formic acid on the catalyst surface. Fig. 5 shows the representative TPO profiles of the MnOx/γ-Al_2O_3 catalyst at low loading level (2.5 wt%) and high loading level (15 wt%) obtained when the catalysts were heated up to 773 K with a heating rate of 10 K/min. Formic acid was observed at low temperature region (350–370 K) for both the catalysts. The COx evolution at low temperature region (first peak) corresponds mainly to the oxidation of weakly bound byproducts on catalyst surface, whereas that at high temperature region (second peak) is due to the strongly bound surface species including surface formates and carboxylates [7].

Table 2 summarizes the peak temperatures and the amount of product compounds on the catalysts estimated from the TPO profiles for the MnOx/γ-Al_2O_3 catalysts with different Mn loadings. The temperature for the second peak decreased with the increase in Mn loadings up to 7.5 wt% and was unchanged at higher loading level, while the temperature for the oxidation of weakly bound species were almost unchanged by changing the Mn loadings. This behavior reflected the catalytic activities of Mn oxides for the oxidation of byproduct compounds on the catalyst. The amount of COx and HCOOH evolved during the TPO profiles was also listed in Table 2. The product distribution was not so much influenced by Mn loadings, further supporting the consideration described above that the oxidation behavior of benzene is very similar for the isolated manganese oxide species and aggregated Mn_3O_4 species on alumina.

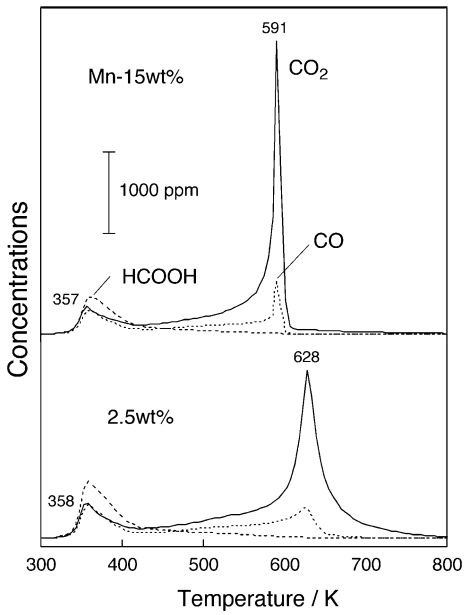

Fig. 5 TPO profiles of the MnOx/γ-Al_2O_3 catalysts after the use for catalytic ozonation of benzene

Table 2 TPO results for MnOx/γ-Al_2O_3 catalysts

Mn loading (wt%)	Temperature (K)[a]		C desorption/C-atom nm^{-2}		
	1st peak	2nd peak	CO_2	CO	HCOOH
1.0	364	655	16.9	8.6	6.0
2.5	358	628	21.5	7.5	6.2
5.0	361	600	17.6	7.1	5.5
7.5	360	589	17.3	6.1	4.8
10.0	358	587	17.8	6.1	5.0
15.0	357	591	18.0	6.1	5.0

TPO measurements were conducted in O_2 flow with a heating rate of 10 K/min

[a] Temperature peak in the profile of COx evolution

4 Conclusion

We studied the benzene oxidation with ozone over alumina-supported manganese oxides with different Mn dispersions. The isolated Mn oxide species and aggregated Mn oxides were formed on alumina by using conventional impregnation technique and changing the Mn loadings. Both the manganese oxide species were active for benzene oxidation. The rate for ozone decomposition to that of benzene oxidation was almost unchanged by changing the Mn loadings. TPO studies indicated that the product distribution on catalyst surface was not influenced by the Mn loadings. These findings suggest that the oxidation behavior of benzene was very similar for the isolated manganese oxide species and aggregated Mn_3O_4 species.

Acknowledgments We are grateful to the approval of Photon Factory Advisory Committee (Proposal No. 2003G071) at High Energy Accelerator Research Organization for the XAFS measurements. This work was conducted at National Institute of Advanced Industrial Science and Technology.

References

1. Hunter P, Oyama ST (2000) Control of volatile organic compound emissions: conventional and emerging technologies. Wiley, New York
2. Andreeva D, Tabakova T, Ilieva L, Naydenov A, Mehandjiev D, Abrashev MV (2001) Appl Catal A 209:291

3. Naydenov A, Mehandjiev D (1993) Appl Catal A 97:17
4. Mehandjiev D, Cheshkova K, Naydenov A, Georgesku V (2002) React Kin Catal Lett 76:287
5. Mehandjiev D, Naydenov A, Ivanov G (2001) Appl Catal A 206:13
6. Einaga H, Futamuara S (2004) React Kin Catal Lett 81:121
7. Einaga H, Futamura S (2004) J Catal 227:304
8. Li W, Oyama ST (1997) Stud Surf Sci Catal 110:873
9. Reed C, Xi Y, Oyama ST (2005) J Catal 235:378
10. Einaga H, Futamura S (2005) Appl Catal B 60:49
11. Li W, Gibbs GV, Oyama ST (1998) J Am Chem Soc 120:9041
12. Li W, Oyama ST (1998) J Am Chem Soc 120:9047
13. Radhakrishnan R, Oyama ST, Chen JG, Asakura K (2001) J Phys Chem B 105:4245
14. Kapteijn F, Singoredjo L, van Driel M, Andreini A, Moulijn JA, Ramis G, Wachs IE (1994) J Catal 150:105
15. Koningsberger DC (1993) Jpn J Appl Phys 32(Suppl 32–2):877
16. Ressler T (1998) J Synchrotron Radiat 5:118
17. Ressler T (1997) J Phys IV 7(No. C2):269
18. Buciuman F, Patcas F, Craciun R, Zahn DRT (1999) Phys Chem 1:185
19. Radhakrishnan R, Oyama ST, Ohminami Y, Asakura K (2001) J Phys Chem B 105:9067
20. Kijlstra WS, Poels EK, Bliek A, Weckhuysen BM, Schoonheydt RA (1997) J Phys Chem B 101:309
21. Xi Y, Reed C, Lee YK, Oyama ST (2005) J Phys Chem B 109:17587
22. Reed C, Lee YK, Oyama ST (2006) J Phys Chem B 110:4207